

Spatiotemporal Evolution of Probe Beams Guided Between Bright Solitons of Nondegenerate Frequencies

A. Dreischuh, E. Eugenieva, and S. Dinev

Abstract— We analyzed an alternative approach for guiding parallel signal beams nested between noninteracting fundamental bright spatial solitons. The numerical results show that stable signal-wave guiding without a cross-talk is obtainable even at small-intensity fluctuations of the control beams ($\pm 10\%$) and at nonperfect alignment of the signal beams with respect to the channels formed by the solitons. Conditions under which the temporal changes of the signal pulses could be asymptotically reduced are discussed.

I. INTRODUCTION

THE CHARACTERISTIC behavior of intense laser beams/pulses in nonlinear optical media has opened up fascinating possibilities for the development of ultrafast all-optical devices. Solitons in optical fibers [1], [2] have been proposed [3] as carriers of information. Solitons of shorter width may provide, in principle, higher bit rates. Unfortunately, the changes of the soliton characteristics limit the use of femtosecond solitons. These changes originate in the higher order dispersion [4], intrapulse Raman scattering [5], the interaction between copropagating solitons [6], the jitter in the pulse arrival [7], and the shock effect [8], etc.

The information capacity of a communication line could be enhanced utilizing a parallel data transmission. One possible scheme involves an interaction of different colored solitons, resulting in a formation of a stable packet of synchronous pulses [9], [10]. The bit order becomes coded in wavelengths, whereas the bit value (zero or unity) is coded in the pulse amplitudes. Optical interconnects for parallel information transmission/processing systems of bandwidths of tens of gigabits per second are under investigation [11].

Far from addressing the particular technical problems of the parallel data transmission, in this work we study numerically the dynamics of signal beams/pulses guided between bright spatial solitons. When CW control beams copropagate in a planar optical waveguide, they can form intermediate channels (i.e., waveguides of nonlinear claddings) in which probe beams/pulses can be guided. To ensure a reasonably extended guiding distance, the control beams should propagate in the form of noninteracting bright spatial solitons. The approach should prevent the cross-talk between the signal beams. The optical alignment of the latter ones is found to not be a critical one. The numerical simulations on the signal beam/pulse

evolution under nonnegligible self-phase modulation indicated the possibility of an asymptotical reproducibility of the signal pulse width and radius to be achieved.

II. PRINCIPLE SCHEME AND PHYSICAL MECHANISMS

The configuration analyzed is depicted in Fig. 1. The nonlinear medium considered is planar. The incoming control beams should propagate inside in the form of noninteracting fundamental bright spatial solitons. The spatial soliton mode of propagation requires an exact compensation of the one-dimensional (1-D) diffraction by the spatial self-phase modulation (SPM) [12], [13]. The control beam diffraction in the perpendicular transverse direction is prevented by a total internal reflection (linear process). A noninteracting mode of propagation of the control beams could be relatively easily obtained by choosing larger beam-to-beam separation, however, it should be kept reasonably small. For two light waves of equal intensities, the criterion for preventing a mutual entrainment and collapse is found to be [14]

$$|2\Delta| > \rho \left[2 \ln \left(\frac{2P}{2P_{\text{crit}} + P} \right) \right]^{1/2} \quad (1)$$

where 2Δ is the initial beam separation, ρ is the beam radii at $1/e$ intensity level, and P_{crit} and P are the critical power for beam self-focusing and the actual power, respectively.

In our interaction configuration, the signal beams/pulses propagate between the control beams. The signal beams/pulses are assumed to be weak and no self-action is accounted for. This assumption is not a principle one and is removed in the last part of this analysis. The probe waves experience the influence of the control beams only. This induced action originates in the spatial refractive-index change along/across the nonlinear medium caused by the control beams. Induced phase modulation (IPM) is the physical process by which a pump field modifies the index of refraction seen by the copropagating probe field [15]. In our model, a negative nonlinear refractive index n_{2s}^{IPM} for IPM of the signal waves is assumed. The propagation of the control beams as spatial bright solitons requires a positive nonlinear index n_{2p}^{SPM} at the control beams' wavelength/polarization. These two requirements could be satisfied for a nonlinear medium with an orientational Kerr effect at different polarizations of the pump and probe waves. Semiconductors or semiconductor-doped glasses offer another possibility for a proper choice of nonlinear refractive indexes n_{2p}^{SPM} , n_{2s}^{IPM} at different wavelengths of the pump and probe

Manuscript received April 20, 1994; revised April 22, 1996.

The authors are with the Department of Physics, Sofia University, BG-1126 Sofia, Bulgaria.

Publisher Item Identifier S 0018-9197(96)06288-4.

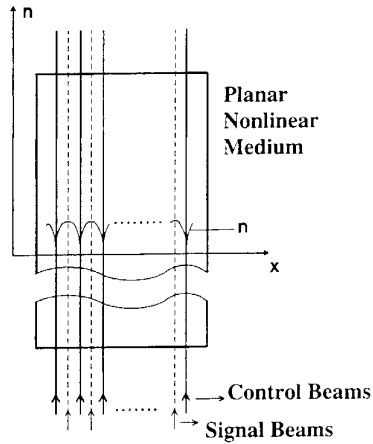


Fig. 1. Principle scheme of the configuration analyzed. CW control beams propagate in a planar optical waveguide in the form of noninteracting bright spatial solitons. They form intermediate channels (i.e., nonlinear waveguides) in which signal pulses could be guided. Spatial distribution of the effective refractive index n seen by the signal waves, is shown also.

waves [16], [30], [31]. Between the control beams, the local refractive index, seen by the signal waves, has a higher value, decreasing as it approaches the control beams. Therefore, two adjacent control beams form a gradient-index nonlinear waveguide for the signal pulses/beams propagating in between. A similar situation arises when a signal wave is guided by dark spatial solitons [17] ($n_{2p}^{\text{SPM}}, n_{2s}^{\text{IPM}} < 0$ for this case) or by bright on-axis spatial solitons [18] ($n_{2p}^{\text{SPM}}, n_{2s}^{\text{IPM}} > 0$). In the latter case, the signal beams are guided inside the bright solitons.

The off-axial propagation of optical beams/pulses under IPM has been studied by a number of authors both theoretically [19]–[21] and experimentally [22]–[24] and seems to be attractive for all-optical switching, pulse-shaping, and shortening [25]–[27].

The cross-talk between the neighboring signal beams could be used as an evaluation criterion for the guiding quality. An eventual symmetrical decrease in the control beam intensity will cause their spatial broadening, which may result in a spatial compression and a peak-intensity enhancement of the signal beams/pulses [28], [29]. Therefore, the undesired cross-talk between the signal beams will be avoided.

In Section IV-A, we concentrate on the spatial behavior of the signal waves involved in the proposed scheme. The temporal behavior of the signal pulses is affected not only by the material's group-velocity dispersion (GVD), but also by the spatial evolution of the signal beam/pulse. An analysis on this problem is presented in Section IV-B, accounting for the possible spatiotemporal self-action (self-phase modulation, SPM) of the signal beams/pulses.

III. NUMERICAL PROCEDURE

In view of the preceding assumptions, the propagation of the control beams along the planar nonlinear medium is described by the nonlinear Schrödinger equation [18], [19]

$$i \frac{\partial \psi_p}{\partial \xi} + \frac{1}{2} \frac{\partial^2 \psi_p}{\partial \eta^2} + |\psi_p|^2 \psi_p = 0 \quad (2)$$

where ψ_p , ξ , and η are the dimensionless beam envelope, propagation distance and transverse, and diffraction unlimited coordinate, respectively. They are related to the physical variables by

$$\xi = \frac{z}{L_{\text{Diff}_P}} \quad (3a)$$

$$\eta = \frac{x}{a_p} \quad (3b)$$

$$\psi_p = k_p a_p \left(\frac{n_{2p}^{\text{SPM}}}{2n_{0p}} \right)^{1/2} A_p \quad (3c)$$

where L_{Diff_P} is the Rayleigh diffraction length ($L_{\text{Diff}_P} = k_p a_p^2$), $k_p = 2\pi/\lambda$, λ is the control-beams wavelength, a_p —their physical radii at $1/e$ intensity level, A_p is the electric field amplitude, and n_{2p}^{SPM} is the nonlinear refractive-index coefficient for SPM at a wavelength λ_p . The spatial soliton mode of propagation requires a self-focusing nonlinear medium (i.e., $n_{2p}^{\text{SPM}} > 0$). The minimum number of control beams of interest in the present numerical model is 3. In this case, for instance, the initial control-beam profiles are assumed to be of sech-form

$$\psi_p(\xi = 0) = \text{sech}(\eta) + \text{sech}(\eta + 2\Delta) + \text{sech}(\eta - 2\Delta) \quad (4)$$

where 2Δ is the initial control-beam separation.

In a pump-probe approximation, accounting for the signal beam diffraction and neglecting the group-velocity dispersion (GVD) (see Section IV-B), the signal beam evolution is described by [18], [19]

$$i \frac{\partial \psi_s}{\partial \xi} + \frac{1}{2} \frac{\lambda_s}{\lambda_p} \frac{\partial^2 \psi_s}{\partial \eta^2} + |\psi_p|^2 \psi_s \text{sgn}(n_{2s}^{\text{IPM}}) \alpha = 0 \quad (5a)$$

where

$$\psi_s = k_s a_s \left(\frac{n_{2s}^{\text{IPM}}}{2n_{0s}} \right)^{1/2} A_s \quad (5b)$$

ψ_s and A_s are, respectively, the dimensionless and the physical electric field amplitudes of the signal beams/pulses of wavelength λ_s , n_{2s}^{IPM} is the nonlinear coefficient accounting for the intensity-dependence of the medium refractive index due to IPM. The coupling coefficient α depends on the nature of the physical process that produces the optical nonlinearity (e.g., molecular orientation, electronic response of bound electrons, etc.) and on the experimental conditions (e.g., the polarizations of the pump and probe waves). For a medium of a nonresonant electronic nonlinearity due to bound electrons, $\alpha = 2$ for parallel polarizations of the pump and probe fields and $\alpha = 2/3$ for crossed polarizations. In media possessing orientational Kerr nonlinearity besides the polarizations of the pump and probe fields, one should take into account both the electronic and molecular contributions to the optical nonlinearity in order to get a more realistic value of α [35]. The input signal beam shapes are assumed to be Gaussian with a_s being their initial physical radii at $1/e$ intensity level. According to the principle scheme described, (5) implies that the interaction between the control and signal waves manifests itself only in the propagation of the signal waves.

The propagation of the control and the signal waves is simulated using the split-step Fourier method [19]. The initial control beams profile given by (4) was used to adjust the control beam-to-beam distance only in order to prevent the soliton interaction. In the scheme performance analysis, however, the evolution of five control beams and four signal beams is simulated. This number was limited by the computer resources available and by the necessity not to overlook relatively weak shape changes. Five control beams show the characteristic ordering of one central soliton beam, intermediate solitons, and two side-lying soliton beams, for which only one neighboring exists. It will be shown later that, even under fundamental soliton mode of the control beam propagation and at a perfect signal beam alignment, the signals are sensitive with respect to their disposition in the sequence.

In Section IV-B, the spatiotemporal evolution of the signal beams/pulses is modeled on the base of the generalized nonlinear Schrödinger equation

$$i \frac{\partial \psi_s}{\partial \xi} + \frac{1}{2} \frac{\partial^2 \psi_s}{\partial \eta^2} + \frac{L_{\text{DiffP}}}{2L_{\text{Disps}}} \text{sgn}(\beta_s) \frac{\partial^2 \psi_s}{\partial \tau^2} + |\psi_s|^2 \psi_s \text{sgn}(n_{2s}^{\text{SPM}}) + |\psi_p|^2 \psi_s \text{sgn}(n_{2s}^{\text{IPM}}) \alpha = 0 \quad (6a)$$

where, further to the notations introduced above, $\tau = t/t_0$ is the dimensionless time, t_0 denotes the signal pulse duration, n_{2s}^{SPM} is the nonlinear refractive index for signal SPM, β_s accounts for the signal GVD [$\text{sgn}(\beta_s) = +1$ means anomalous GVD], and $L_{\text{Disps}} = t_0^2/|\beta_s|$ is the corresponding dispersion length. Instead, by (5b), the dimensionless and the physical electric field amplitudes ψ_s and A_s are related by

$$\psi_s = k_s a_s \left(\frac{n_{2s}^{\text{SPM}}}{2n_{0s}} \right)^{1/2} A_s. \quad (6b)$$

For simplicity, $|\lambda_s - \lambda_p| \ll \lambda_{s,p}$ and $a_s/a_p \approx 1$ are assumed, which seems reasonable at this stage of the analysis. The control beams are assumed to remain unaffected by the cross-phase modulation originating from the signal wave (2) for two reasons. First, only the wings of the control and signal beams overlap. Second, as we will show later, the signal-pulse duration stops increasing and starts oscillating around its initial value at a signal-pulse peak intensity, which is $\sim 30\%$ of the control-beam intensity.

The four-wave mixing effects occurring in materials possessing fast nonlinearities are not accounted in the models (2), (5a), and (6a). At control and signal waves at different wavelengths, provided that the planar waveguide length is much greater than the coherence length, their contribution should be negligible.

IV. NUMERICAL RESULTS AND DISCUSSION

A. Spatial Aspects

As a first step, we tested our programs against the reproducibility of results of other authors. We simulated one fundamental soliton formation and the periodic collapse of a soliton pair along a nonlinear medium due to mutual interaction [15]. The stability of the guiding mode analyzed requires a noninteracting regime of propagation of the control

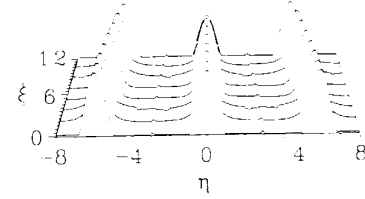


Fig. 2. Undesired interaction between the parallel control beams along the nonlinear medium. The mutual attraction depends on the soliton separation.

beams. It should be noted that their higher number results in a more complicated evolution. For three control beams, we found (Fig. 2) that at a beam-to-beam distance $x_0 = 1.25(2\Delta)$ (i.e., $x_0 = 6a_p$), a mutual attraction is still presented. Stable propagation over $\xi = 25$ was found at $x_0 = 1.75(2\Delta)$ ($x_0 = 8.24a_p$). The higher value obtained for the off-axial control-beam separation required is probably due to the Gaussian beam profiles considered in deriving (1) [14]. At the same value of the control-beam offset, a stable propagation of five waves was also found.

Successive performance of the guiding scheme analyzed could be claimed out only at no cross-talk between the signal beams. We observed stable guiding and periodic oscillations of the signal waves at $\text{sgn}(n_{2s}^{\text{IPM}}) = -1$, i.e., the nonlinear medium should be self-focusing, but induced-defocusing. Such a situation, in principle, could be obtained at $\lambda_s \neq \lambda_p$ ($|\lambda_s - \lambda_p| \ll \lambda_{s,p}$) in semiconductor-doped glasses. The polarization-dependence of the sign of the orientational Kerr nonlinearity is well known, but it does seem to be of practical interest in proof-of-principle experiments only.

The evolution of the signal beams is presented on Figs. 3 and 4. The control-beam profiles at the entrance of the nonlinear waveguide are assumed to be of the form

$$u_p(\xi = 0) = \text{sech}(\eta + 2x_0) + \text{sech}(\eta + x_0) + \text{sech}(\eta) + \text{sech}(\eta - x_0) + \text{sech}(\eta - 2x_0). \quad (7)$$

The signal-beam profiles are assumed to have a Gaussian form, equal radii a_s at $1/e$ intensity level, and $a_s/a_p = 1.3$ is assumed for the case analyzed. In Fig. 3, an initial signal-beam broadening followed by periodic oscillations is clearly seen. In Fig. 4(a), the signal-beam profiles are depicted at $\xi = 4$ (dashed line) and $\xi = 20$ (dots). These profiles correspond to the first and the last expansion of the signal beams in Fig. 3. The solid lines represent the input signal-beam profiles. It is important to note that there is no cross-talk between the signals. Fig. 4(b) represents the signal-beam profiles at $\xi = 8$ (dashed line) and $\xi = 24$ (dots), which correspond to the first and the last spatial narrowing of the signal waves (see Fig. 3). It can be seen that the profiles are practically the same at the first and the last signal-beam narrowing, differing slightly from the initial signal-beam profiles. The comparison between the side-lying and the middle-lying beams shows that even at perfect initial conditions, the signal-beam profiles are slightly sensitive with respect to the beam disposition. That fact, however, does not significantly disturb the guiding mode analyzed.

Further, it is important to estimate the stability of the scheme against small-intensity fluctuations of the control beams. Fig. 5

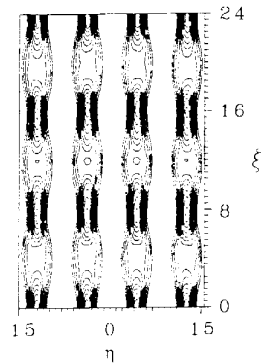
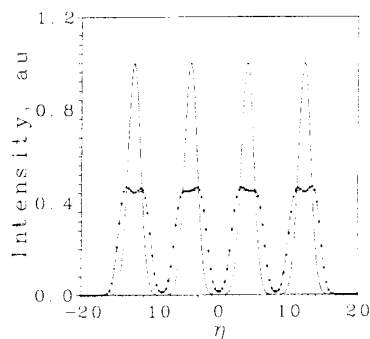
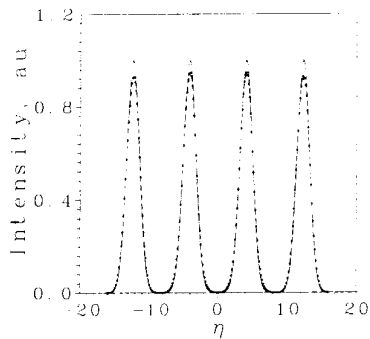


Fig. 3. Spatial evolution of the signal beams along the nonlinear medium. Periodic oscillations of the signal-beam radii are clearly seen.



(a)



(b)

Fig. 4. (a) Signal-beam profiles at the first (dashed lines) and the last (dots) expansion modeled. The solid lines represent the signal-beam profiles at the entrance of the nonlinear waveguide. The absence of a cross-talk between the signal beams is evident. (b) Signal-beam profiles at the first (dashed lines) and the last (dots) narrowing modeled.

gives an idea on the peak intensities of the control beams assumed in the stability analysis, normalized to the peak intensity of the fundamental bright soliton. Fig. 6 shows the resulting evolution of the signal beams along the nonlinear medium. Periodic oscillations, similar to those depicted in Fig. 3 for the ideal case, can be observed. It is worth noting that the first and the last expansion (narrowing, respectively) occur approximately at the same distances as in the ideal case for which the control beams propagate in the form of first-order bright spatial solitons. The spatial signal-beam profiles

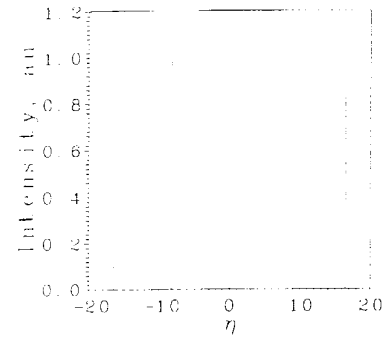


Fig. 5. Initial disposition scheme of the intensity fluctuating control beams assumed in generating Fig. 6.

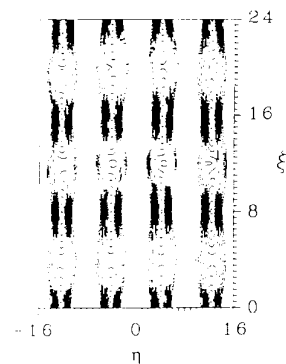


Fig. 6. Influence of the fluctuations in the control-beam intensities ($\pm 10\%$) on the signal-beam propagation. Periodic oscillations are clearly expressed.

at those characteristic distances are almost the same as those depicted in Fig. 4 and there is no cross-talk between the signal beams. It is shown [30] that a stationary regime of control-beam propagation should exist at a consecutive arrangement of beams of higher and lower intensities. In view of the present results, under such an arrangement the signal beams/pulses should be guided without a cross-talk over longer distances or even closely spaced across the waveguide.

Our analyses showed that periodic oscillations without a cross-talk can be observed also at a nonperfect alignment of the signal beams with respect to the centers of the channels formed. Fig. 7 gives an idea on the relative positions of the signal beams' centers at the entrance of the nonlinear waveguide in this case. The maximum initial deviation from the channel center is 25% the channel half-width (i.e., the initial distance between the centers of the control and signal beams is not less than $3a_p$). The control-beam profiles have the form given by (7). The spatial evolution of the signal beams obtained under these conditions is plotted on Fig. 8. Periodic oscillations in the signal-beam radii, similar to those which should be expected under perfect initial conditions (Fig. 3) and at weak-intensity fluctuations of the control beams (Fig. 6), are clearly seen. The period of the oscillations, however, is increased. The nonlinear waveguide induced by the control beams (with a gradient-index change and a nonlinear cladding) "reflects" back the signal wave and no cross-talk is evident. Fig. 9(a) presents the signal-beam profiles at $\xi = 5$

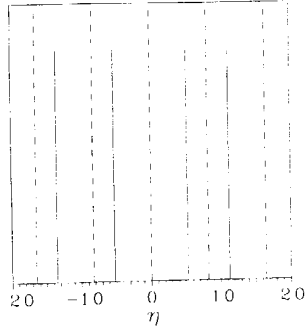


Fig. 7. Initial disposition scheme of the signal beams (solid lines) with respect to the control beams (dashed lines) used in generating Figs. 8 and 9.

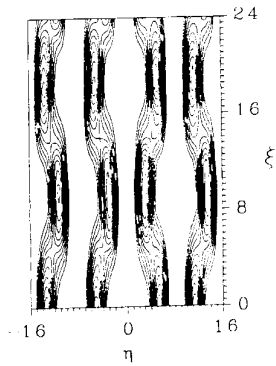
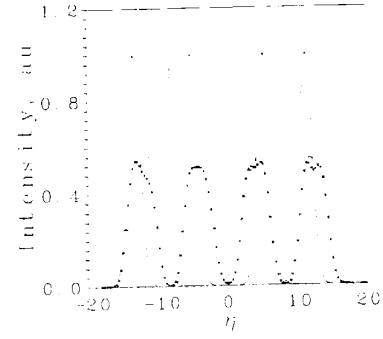


Fig. 8. Spatial evolution of the signal beams when they are not perfectly aligned with respect to the information channels (offset $\pm 10\%$). A stable waveguiding is clearly expressed.

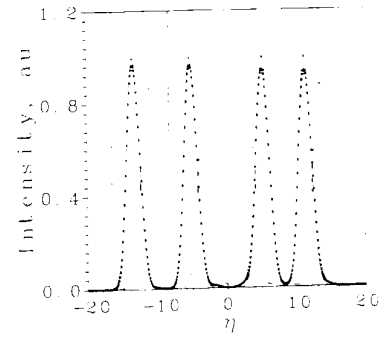
(dashed lines) and $\xi = 14$ (dots), which corresponds to the first and the last spatial broadening of the signal beams. The solid curves correspond to the initial beam profiles. It is interesting to note that the signal beams appear to be centered with respect to the intermediate nonlinear channels when their broadening is the highest one. This broadening, however, results in signal-beam intensities of approximately 10% higher as compared to the perfect situation and the case with control-beam peak-power fluctuations [see Fig. 4(a)]. Fig. 9(b) shows the signal-beam profiles at $\xi = 9$ (dashed curve) and $\xi = 18$ (dotted curve). It should be noted that a maximum spatial signal-beam narrowing appears periodically in two cases—at a maximum and at a minimum signal-beam deflection with respect to the input signal beam [Fig. 9(b), solid curve]. Nevertheless, even at a 25% signal-beam misalignment with respect to the channel centers, no cross-talk is observed.

B. Spatiotemporal Aspects

It is natural to expect that the influence of the complicated 1-D (spatial) evolution of the signal beams (Figs. 3, 4, 6, 8, and 9) on the temporal behavior of the signal pulses will not be a negligible one. We modeled the spatiotemporal evolution of a single signal beam/pulse localized between two control beams. In the notations introduced above, (6a) is solved at $a_s/a_p = 1$ and $x_0 = 8a_p$. The initial signal-pulse profile is assumed to be Gaussian with a duration of t_0 . In order



(a)



(b)

Fig. 9. (a) Signal-beam profiles at the first (dashed lines) and the second (dots) expansion. The solid lines represent the signal-beam profiles at the entrance of the nonlinear waveguide. Vertical lines indicate the position of the control beams. (b) Signal-beam profiles at the first (dashed lines) and the second (dots) narrowing.

to avoid a complete signal spatiotemporal symmetry at the entrance of the nonlinear medium, the GVD coefficient $|\beta_s|$ is scaled to ensure that one dispersion length $\zeta = L_{\text{Disp}_s}$ is equal to four Rayleigh diffraction lengths ξ . Assuming no initial chirp of the signal pulse, in the linear regime of propagation a monotonic signal pulse broadening ($\sqrt{2}$ times at $\zeta = 1$) should be expected. The main tendency observed was really such a dispersive broadening of the signal, but it was modulated periodically. This purely linear evolution is qualitatively similar to the evolution of the signal pulse [Fig. 10(a)] under a SPM, 10 times weaker than the spatial SPM of the control beams. The weak SPM of the signal at $n_{2s}^{\text{SPM}} > 0$ in the anomalous GVD regime ($\beta_s < 0$) leads to a slight reduction of the signal temporal broadening and to a slightly enhanced spatial signal-beam spreading [Fig. 10(b)] at the distances of maximum expansion (see Fig. 3). This spatial spreading increases with increasing the signal intensity up to 30% the intensity of the control beams [Fig. 10(d)]. At this signal level, as a mean, the signal pulse duration retains its initial value [Fig. 10(c)]. The coupling between the spatial and the temporal dimensions of the signal beam/pulse is evident. The maximum signal spreading in space [at $\xi \sim 1$ and $\xi \sim 3.4$, Fig. 10(b) and (d)] leads to a corresponding pulse shortening [Fig. 10(a) and (c)]. The opposite seems obvious at $\xi \sim 2.2$. It should be noted that under these conditions the signal SPM and the IPM from the control beams could lead to an asymptotical reproducibility of the signal-beam width and

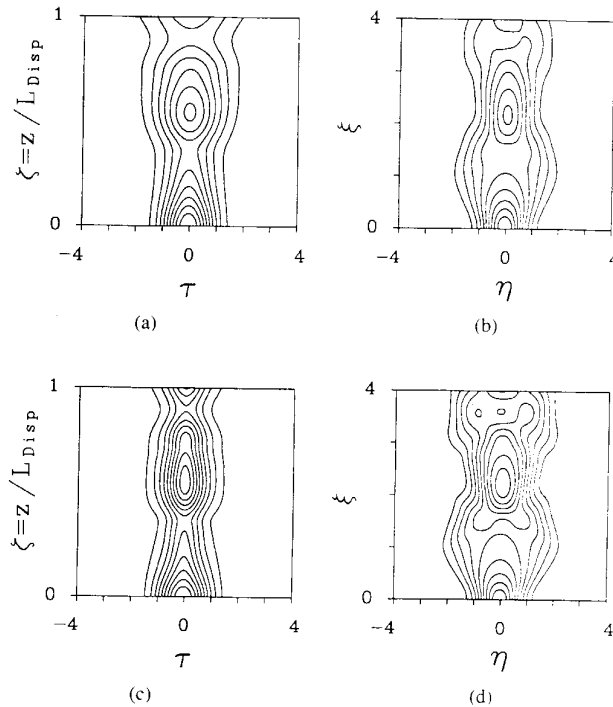


Fig. 10. (a), (c) Temporal and (b), (d) spatial evolution of a signal beam/pulse of a low and moderate peak intensity (0.1 and 0.3 times the control-beam intensity, respectively). One dispersion length ζ corresponds to four diffraction lengths ξ .

of the signal-pulse duration without a cross-talk between the adjacent waves.

V. CONCLUSION

In conclusion, the parallel guiding of signal beams/pulses seems to be feasible between bright solitons of nondegenerate frequencies. The numerical simulations show that a relatively stable signal-beam guiding without a cross-talk is to be expected not only at perfect initial conditions (fundamental bright spatial solitons as control beams and perfect alignment of the signal beams) but also at relatively small-intensity fluctuations of the control beams ($<\pm 10\%$) and at a nonperfect alignment of the signal beams with respect to the written channels ($<25\%$). The spatiotemporal behavior of the signal waves is analyzed on the base of the generalized nonlinear Schrödinger equation (6a). The numerical results show that in a planar self-focusing and induced-defocusing nonlinear medium of a negative GVD at the signal wavelength, an asymptotic reproduction of the signal spatial width and temporal duration could be achieved.

This sign combination of the nonlinear refractive indexes required is available in Kerr nonlinear media with an orientational effect at a perpendicular polarization of the control wave with respect to the signal one. At nondegenerate control and signal frequencies, it could be obtained in zinc-blend semiconductors [31], in glass composites [32], or in photorefractive media [33]. The two-photon absorption and the four-wave mixing effects were neglected in this analysis, however they may influence the signal guiding and require future analyses. Attention should be paid also to the possible controllable

steering of the control beams [34] and on the associated evolution changes of the signal waves.

REFERENCES

- [1] A. Hasegawa and F. Tappert, "Transmission of stationary nonlinear optical pulses in dispersive dielectric fibers I—Anomalous dispersion," *Appl. Phys. Lett.*, vol. 23, pp. 142–144, 1973.
- [2] L. F. Mollenauer, R. H. Stolen, and J. P. Gordon, "Experimental observation of picosecond pulse narrowing and solitons in optical fibers," *Phys. Rev. Lett.*, vol. 45, pp. 1095–1098, 1980.
- [3] A. Hasegawa and Y. Kodama, "Signal transmission by optical solitons in monomode fiber," *Proc. IEEE*, vol. 69, pp. 1145–1150, 1981.
- [4] P. K. A. Wai, C. R. Menyuk, Y. C. Lee, and H. H. Chen, "Nonlinear pulse propagation in the neighborhood of the zero-dispersion wavelength of monomode optical fibers," *Opt. Lett.*, vol. 11, pp. 464–466, 1986.
- [5] K. J. Blow, N. J. Doran, and D. Wood, "Suppression of the soliton self-frequency shift by bandwidth-limited amplification," *J. Opt. Soc. Amer. B*, vol. 5, pp. 1301–1304, 1989.
- [6] J. P. Gordon, "Interaction forces among solitons in optical fibers," *Opt. Lett.*, vol. 8, pp. 596–598, 1983.
- [7] L. F. Mollenauer, M. J. Neubelt, S. G. Evangelides, J. P. Gordon, J. R. Simpson, and L. G. Cohen, "Experimental study of soliton transmission over more than 10,000 km in dispersion shifted fiber," *Opt. Lett.*, vol. 15, pp. 1203–1205, 1990.
- [8] W. Zhao and E. Bourkoff, "Femtosecond pulse propagation in optical fibers: Higher order effects," *IEEE J. Quantum Electron.*, vol. 24, pp. 365–372, 1988.
- [9] V. V. Afanasiev, L. M. Kovachev, and V. N. Serkin, "Mixed states of optical solitons at different wave lengths," *JETP Lett.*, vol. 16, pp. 10–14, 1990 (in Russian).
- [10] L. M. Kovachev, "Influence of cross-phase modulation and four-photo parametric mixing on the relative motion of optical pulses," *Opt. Quantum Electron.*, vol. 23, pp. 1091–1102, 1991.
- [11] M. Shimazu, "DARPA funds \$8 million consortium to pursue optical backplane interconnect," *Photon. Spectra*, vol. 26, no. 9, pp. 28–30, Sept. 1992.
- [12] J. S. Aitchison, A. M. Weiner, Y. Silberberg, M. K. Oliver, J. L. Jackel, D. E. Leaird, E. M. Vogel, and P. W. Smith, "Observation of spatial optical solitons in nonlinear glass waveguide," *Opt. Lett.*, vol. 15, pp. 471–473, 1990.
- [13] J. S. Aitchison, Y. Silberberg, A. M. Weiner, D. E. Leaird, M. K. Oliver, J. L. Jackel, E. M. Vogel, and P. W. E. Smith, "Spatial optical solitons in planar glass waveguide," *J. Opt. Soc. Amer. B*, vol. 8, pp. 1290–1297, 1991.
- [14] C. J. McKinstrie and D. A. Russel, "Nonlinear focusing of coupled waves," *Phys. Rev. Lett.*, vol. 61, pp. 2929–2932, 1988.
- [15] G. P. Agrawal, *Nonlinear Fiber Optics*. Boston, MA: Academic, 1989, pp. 105–146 and 173–215.
- [16] M. Sheik-Bahae, D. C. Hutchings, D. J. Hagan, and E. W. Van Stryland, "Dispersion of bound electronic nonlinear refraction in solids," *IEEE J. Quantum Electron.*, vol. 27, pp. 1296–1309, 1991.
- [17] C. T. Law and G. A. Swartzlander, "Wave guiding by optical-vortex soliton arrays," in *Proc. QELS'95*, paper QTuD4, p. 45.
- [18] R. de la Fuente and A. Barthelemy, "Spatial soliton-induced guiding by cross-phase modulation," *IEEE J. Quantum Electron.*, vol. 28, pp. 547–554, 1992.
- [19] G. P. Agrawal, "Induced focusing of optical beams in self-defocusing nonlinear media," *Phys. Rev. Lett.*, vol. 64, pp. 2487–2490, 1990.
- [20] S. Dinev, A. Dreischuh, and I. Ivanova, "Induced deflection of optical beams in an off-axis geometry," *J. Mod. Opt.*, vol. 39, pp. 667–671, 1992.
- [21] ———, "Spatio-temporal analysis of all-optical streaking," *Appl. Phys.*, vol. B56, pp. 34–38, 1993.
- [22] A. Stenz, M. Kauranen, J. Maki, G. P. Agrawal, and R. Boyd, "Induced focusing and spatial wave-breaking from cross-phase modulation in a self-defocusing medium," *Opt. Lett.*, vol. 17, pp. 19–24, 1992.
- [23] J. Hickman, A. Gomes, and C. De Aranjó, "Spatial cross-phase modulation effects in a self-defocusing medium," in *Proc. IQEC'92*, paper ThC6, p. 358.
- [24] J. U. Kang, G. I. Stegeman, and A. S. Aitchison, "Interaction of a weak probe beam with a bright spatial soliton in an AlGaAs planar waveguide," in *Proc. QELS'95*, paper QTuH4, pp. 77–78.
- [25] A. Barthelemy, C. Froehly, S. Maneuf, and F. Reynaud, "Experimental observation of beam's self-deflection appearing with two-dimensional spatial soliton propagation in bulk Kerr material," *Opt. Lett.*, vol. 17, pp. 844–846, 1992.

- [26] A. Dreischuh, E. Eugenieva, and S. Dinev, "Pulse shaping and shortening by spatial filtering of induced-phase modulated probe wave," *IEEE J. Quantum Electron.*, vol. 30, pp. 1656–1661, 1994.
- [27] I. Buchvarov, A. Dreischuh, A. Iliev, S. Dinev, and S. Saltiel, "Simultaneous shaping and shortening of nanosecond pulses," *Proc. SPIE*, vol. 2772, pp. 152–157, 1996.
- [28] Q. Z. Wang, P. P. Ho, and R. R. Alfano, "Effect of DFWM on pulse amplification and compression in the degenerate cross-phase-modulation process," *Opt. Lett.*, vol. 16, pp. 496–498, 1991.
- [29] R. Jin, M. Liang, G. Khitrova, H. M. Gibbs, and N. Peyghambarian, "Compression of bright optical pulses by dark solitons," *Opt. Lett.*, vol. 18, pp. 494–496, 1993.
- [30] I. M. Uzunov, V. D. Stoev, and T. Tzoleva, "N-soliton interaction in trains of unequal soliton pulses in optical fibers," *Opt. Lett.*, vol. 17, pp. 1417–1428, 1992.
- [31] D. C. Hutchings and B. S. Wherrett, "Polarization dichroism of nonlinear refraction in zinc-blende semiconductors," *Opt. Commun.*, vol. 111, pp. 507–512, 1994.
- [32] H. Ma, A. S. L. Gomes, and C. B. de Araujo, "Infrared nonlinearity of commercial Cd(S, Se) glass composites," *Opt. Commun.*, vol. 87, pp. 19–22, 1992.
- [33] M. Morin, G. Durec, G. Salamo, and M. Segev, "Waveguides formed by quasisteady-state photorefractive spatial solitons," *Opt. Lett.*, vol. 20, pp. 2066–2069, 1995.
- [34] X. D. Chao, D. D. Mayerhofer, and G. P. Agrawal, "Optimization of optical beam steering in nonlinear Kerr media by spatial phase modulation," *J. Opt. Soc. Amer. B*, vol. 11, pp. 2224–2231, 1994.
- [35] R. W. Boyd, *Nonlinear Optics*. San Diego, CA: Academic, 1992.
- A. Dreischuh**, photograph and biography not available at the time of publication.
- E. Eugenieva**, photograph and biography not available at the time of publication.
- S. Dinev**, photograph and biography not available at the time of publication.